



HAL
open science

Two Distinct Neuronal Populations in the Rat Parafascicular Nucleus Oppositely Encode the Engagement in Stimulus-driven Reward-seeking

Mehdi Sicre, Frederic Ambroggi, Julie Meffre

► To cite this version:

Mehdi Sicre, Frederic Ambroggi, Julie Meffre. Two Distinct Neuronal Populations in the Rat Parafascicular Nucleus Oppositely Encode the Engagement in Stimulus-driven Reward-seeking. *Current Neuropharmacology*, 2024, 22 (9), pp.1551 - 1565. <10.2174/1570159x22666240131114225>. <hal-04791678>

HAL Id: hal-04791678

<https://hal.science/hal-04791678v1>

Submitted on 19 Nov 2024

HAL is a multi-disciplinary open access archive for the deposit and dissemination of scientific research documents, whether they are published or not. The documents may come from teaching and research institutions in France or abroad, or from public or private research centers.

L'archive ouverte pluridisciplinaire **HAL**, est destinée au dépôt et à la diffusion de documents scientifiques de niveau recherche, publiés ou non, émanant des établissements d'enseignement et de recherche français ou étrangers, des laboratoires publics ou privés.



HAL Authorization

Two distinct neuronal populations in the rat parafascicular nucleus oppositely encode the engagement in stimulus-driven reward-seeking

Mehdi Sicre¹, Frederic Ambroggi^{1,2} and Julie Meffre^{1,2}

¹Aix-Marseille Université, CNRS, Laboratoire de Neurosciences Cognitives, UMR 7291, Marseille, France.

²These authors contributed equally to this work.

Corresponding author: Julie Meffre
Laboratoire de Neurosciences Cognitives
UMR CNRS 7291 – Aix-Marseille Université
3, Place Victor Hugo, Case C
13331 Marseille Cedex 3, France
Office: +33 (0)4 13 55 09 37
Fax: +33(4)13 55 09 58
Email: meffrejulie@gmail.com

ABSTRACT

The thalamus is a phylogenetically well-preserved structure. Known to densely contact cortical regions, its role in the transmission of sensory information to the striatal complex has been widely reconsidered in recent years. The parafascicular nucleus of the thalamus (Pf) has been implicated in the orientation of attention towards salient sensory stimuli. In a stimulus-driven reward-seeking task, we sought to characterize the electrophysiological activity of Pf neurons in rats. We observed a predominance of excitatory over inhibitory responses for all events in the task. Neurons responded more strongly to the stimulus compared to lever-pressing and reward collecting, confirming the strong involvement of the Pf in sensory information processing. The use of long sessions allowed us to compare neuronal responses to stimuli between trials when animals were engaged in action and those when they were not. We distinguished two populations of neurons with opposite responses: MOTIV+ neurons responded more intensely to stimuli followed by a behavioral response than those that were not. Conversely, MOTIV- neurons responded more strongly when the animal did not respond

to the stimulus. In addition, the latency of excitation of MOTIV- neurons was shorter than that of MOTIV+ neurons. Through this encoding, the Pf could perform early selection of environmental stimuli transmitted to the striatum according to motivational level.

INTRODUCTION

The historic view of the thalamus as a group of nuclei relaying sensory information to the cortex [1] has largely been reevaluated. The thalamus is a phylogenetically ancient structure that evolved before the expansion of the neocortex [2]. Thus, while thalamic nuclei have long been known to provide essential information to the cerebral cortex, it is not surprising that they also intensely connect subcortical regions [3,4]. In particular, the associative thalamic nuclei from the midline and intralaminar group send strong projections to the striatal complex [5]. This structure is considered the entry station of the basal ganglia, a subcortical network participating in the selection and the control of voluntary actions [6,7]. This pattern of connectivity has challenged a key element of the classical model of the basal ganglia stating that the input signal to the striatum originates from the cerebral cortex [8]. Some authors even radically proposed that the thalamus, rather than the cortex, may be the dominant source of sensory information to the basal ganglia [9–11]. This appreciation of thalamic afferents to the striatum has largely incentivized their investigation at the cellular and network levels [12–15] and several studies have now begun to address their functional implications at the behavioral level [16–21].

The primate center médian (CM)/parafascicular (Pf) complex within the caudal intralaminar nuclei has attracted a lot of attention. The CM is not present in the rodent brain but it has been largely documented that the primate CM/Pf complex is equivalent to the rodent Pf [22–24]. There is an extensive topographic projection from the medio-lateral axis of the Pf to a ventromedial-dorsolateral axis of the striatal complex in both rats [5,25,26] and mice [15]. The medial Pf projects to the ventral region of the striatum (i.e. nucleus accumbens, NAc) while the lateral Pf projects to the dorsolateral striatum. A similar topography has also been described in primates [22,23,27].

Electrophysiological recordings have shown that primate CM/Pf neurons are rapidly excited by stimuli from a variety of sensory modalities (auditory, visual and somatosensory). These activations depend on the temporal unpredictability of stimuli and their association with

rewards [16], suggesting that the CM/Pf is involved in attentional orienting toward salient sensory stimuli [28,29]. Furthermore, it has been reported that CM/Pf neurons are more excited by stimuli predicting a small reward compared to a large reward [30] and that the magnitude of these excitations inversely correlates with reaction times [31].

Thus, the CM/Pf could provide important information to the striatum to adequately control task engagement in response to temporally unexpected reward-predictive stimuli. To our knowledge, the response of Pf neurons to reward-predictive stimuli has not been investigated in rodents. The aim of this study was to fill this gap by recording single-neuron activity in the rat Pf during a reward-seeking task. In this task, rats were rewarded for performing an instrumental action in response to a predictive stimulus. We used long sessions to compare Pf neuronal responses to stimuli when rats engaged themselves in reward-seeking and responses when they did not. We found a population of neurons that responded more intensely to reward-predicting stimuli when the animals subsequently engaged in the task compared to when they did not. A second population, which responded to stimuli at shorter latency, had an opposite pattern of activity. We propose that these two populations may respectively allow animals to participate in or refrain from active engagement in response to reward-predictive stimuli through their connections to the NAc.

EXPERIMENTAL PROCEDURES

Subjects

Experiments were conducted on male Long-Evans rats (Charles Rivers, France) weighing ~300 g on arrival. Rats were immediately housed individually on a 12 h light/dark cycle. Experiments were conducted during the light phase. After one week of habituation, rats were placed under food restriction; food rations were adjusted daily to maintain the body weight at ~90% of their free-feeding body weight. All experiments were performed in accordance with the guidelines on animal care and use of the European guidelines (European Community Council Directive, 2010/63/UE) and National guidelines.

Training

All experiments were conducted in operant chambers containing two house lights, a tone speaker, a retractable lever and a reward receptacle located on one wall of the chamber (Med Associates, Vermont, USA). A fan generated a background noise (~60 dB). Liquid sucrose (10 %) was delivered as a reward in the receptacle by a syringe pump. During the first 2 days, rats were trained to obtain 50 μ l of sucrose by spontaneously entering the reward receptacle. When 300 rewards were obtained within an hour, rats were run on a fixed-ratio 1 (FR1) schedule with a 10 s-time-out: the lever was constantly extended in the chamber and a lever-press triggered the delivery of 50 μ l of sucrose into the receptacle. When rats reached the criterion >100 lever-presses within an hour, they were advanced to the stimulus-driven reward-seeking task.

Stimulus-driven reward-seeking task

Rats were run daily on the task for 3 hours. The extension of a lever was used as an auditory/visual instructive stimulus. The lever was extended in the cage in 300 ms via a motor that generated a noise. Because the motors generated different noise levels in the 3 recording cages used for this study, we coupled the extension with a 300 ms/85 dB speaker-generated white noise. When the lever was extended, rats had 10 s to press it to obtain the reward. Each trial was followed by a variable interval schedule averaging 45 s (from 30 to 60 s). If the rats did not lever-press within 10 s, the lever retracted and the intertrial interval was re-initialized. Surgery was performed when rats reached the criterion of >80 % responses during the first hour of the session.

Surgery

Rats were anesthetized with 5% isoflurane and placed in a stereotaxic apparatus (Kopf Instruments, California, USA). Animals received an injection of buprenorphine (0.05 mg/kg, Vetergesic, France) and anesthesia level was adjusted with 0.5-2 % isoflurane during the maintenance phase. Before skin incision, a subcutaneous injection of lidocaine (1mg/ml, Lurocaine MedVet,) was performed. Bundles of 8 electrodes were attached to custom-made microdrives [32] that allowed to lower the electrodes bundles by 80 μ m increments. Electrodes were implanted in the Pf bilaterally in 5 animals and unilaterally in 2 animals (one on the left and the other on the right hemisphere) at the following stereotaxic coordinates:

AP: -4.1, ML: +/-1, DV: -5.4 mm relative to the Bregma. The microdrives and the connectors were secured to the skull with bone screws, adhesive cement (C&B Metabond, Phymep, France) and dental acrylic (Phymep, France). After surgery, a prophylactic analgesic treatment (Buprenorphine, 0.05 mg/kg, Vetergesic, France) was administered, and rats were given at least 7 days of recovery with *ad libitum* access to food. After recovery, rats were placed in food restriction and re-trained until reaching previous criteria.

Electrophysiology

Recording procedure

Electrophysiological recordings were conducted as described previously [33] during 3 hour-long sessions. Animals were connected to the electrophysiological acquisition system (SpikeGadget LLC, California, USA). The 32-channel headstage, streaming data at 30 kHz per channel, was connected to a low-torque HDMI commutator that allowed the animals to be free of their movements in the chamber. Between sessions, electrodes bundles were lowered by 80 or 160 μm increments to record new set of neurons. Unfiltered data were transferred from the data acquisition main control unit to a data acquisition computer where it was visualized and saved. Digitally-filtered data (0.2-6 kHz) were used for spike sorting.

Spike sorting

Recorded data were analyzed with OfflineSorter (Plexon Inc, Texas, USA) to isolate spikes from single neurons with principal component analysis. Inter-spike interval distributions, cross-correlograms and auto-correlograms were used to ensure that the activity of single neurons was isolated. Only well isolated waveforms with characteristics that were constant over the entire recording session were included in this study. Sorted units were exported to NeuroExplorer 4.135 (Nex Technologies, Colorado, USA) and Matlab R2022b (MatWorks Inc, Massachusetts, USA) for further analysis.

Electrophysiological analyses

Waveform Analysis

In our data set, 290 neurons showed waveforms with a negative followed by a positive deflection. The remaining 95 neurons displayed the opposite pattern. The spike width was

assessed by the time elapsed between the first and second extremum independently from the sign of the first and second deflections. The spike width of 14 neurons could not be determined due to technical issues and we then excluded them from the analyses involving this parameter.

Responses detection

Peri-stimulus time histograms (PSTHs) were constructed with smoothed (lowess method, span=4) 20 ms- and 2 ms-time-bins. PSTHs constructed around the behavioral events (stimulus presentation, lever-press and reward collection) were used to detect excitations and inhibitions and the time at which they occurred. The 10 s period before the presentation of the stimulus was used as a baseline period. Excitation and inhibition to each event was determined by the presence of at least 3 consecutive bins above the 99 % (for excitations) or below the 1 % (for inhibitions) confidence interval of the baseline during the analysis windows (0 to 250 ms after the stimulus, -2 to 1 s around lever-presses and reward delivery). Onset was determined by the time of the first of 3 consecutive bins falling outside the confidence interval. The offset was determined in analogy, by searching the first of 6 consecutive bins within the confidence interval.

Deconvolution

To isolate the activity of temporally close events, we used a deconvolution method as described previously [34,35]. Briefly, the model assumes that the total firing rate of a neuron in each trial is equal to the linear sum of the contributions of each event-related firing, delayed by the event latency in that trial. Here, we deconvolved single event responses for each neuron using the optimal number of iterations that had a cross validation error lower than the PSTHs.

Data normalization and plotting

Color-coded maps and average PSTHs across neurons were constructed with 20 ms- and 2 ms-bins. Prior to averaging, the firing rate of each neuron during each bin was z-score-transformed: $(F_i - F_{\text{mean}})/F_{\text{sd}}$ where F_i is the firing rate of the i^{th} bin of the PSTH, and F_{mean} and F_{sd} are, respectively, the mean and the SD of the firing rate during the 10 s preceding stimulus onset.

Statistical analyses

We sought to compare the trials to which the animal engaged in reward-seeking with those it did not. Thus, we selected the sessions containing at least 20 trials of each type to conduct a reliable analysis of the neuronal data. For behavioral analyses, the primary dependent variables were the percentage of responding to the stimulus and the latency to lever-press after the presentation of the stimulus.

For electrophysiological data, the primary dependent variables were the baseline firing rate, the maximal frequency reached (measured by averaging the top 5% of instantaneous frequencies during the baseline period), the coefficient of variation (measured during the baseline period), the spike width, the proportion of responsive neurons, the mean z-score normalized firing (0-250 ms post-stimulus and -2 to 1 s around lever-presses and reward collection), the onset latency and the durations of the responses. These variables were analyzed with paired, unpaired t-tests or ANOVAs. When appropriate, a Bonferroni test was used to conduct post-hoc comparisons. Proportions were analyzed with χ^2 tests and distributions with Kolmogorov-Smirnov tests. All results were considered significant at $p < 0.05$. Data are presented as mean \pm SEM.

Histology

Animals were euthanized and each electrodes site was labeled by passing a 20 μ A DC current for 7 s. Rats were perfused intracardially with phosphate buffered saline following by 10 % formalin solution. Brains were removed, post-fixed in 10 % formalin and placed in 30 % sucrose for 3 days. Brains were sectioned at 40 μ m on a cryostat and slices were stained with cresyl violet. Reconstruction of the recording sites was made based on the final location of the electrodes.

RESULTS

Behavioral analysis

Rats performed a stimulus-driven task where a compound auditory/visual stimulus was presented unexpectedly (on average every 45 s). The stimulus was a 300 ms-white noise

coupled to the extension of a lever lasting up to 10 s (see methods for details). A lever-press triggered the immediate delivery of a 10 % sucrose reward in an adjacent receptacle and the retraction of the lever (Fig. 1A, B). We sought to analyze neuronal activity when the rats attended to the stimulus and when they did not. In order to obtain a sufficient number of trials of each type, we ran 3-hour long sessions. For all rats, the percentage and latency of lever-pressing in response to the reward-predictive stimulus were variable across sessions (5 to 9 sessions per rat for 7 rats, total of 46 sessions Fig. 1C). Overall, the mean response percentage was 60.9 ± 2.8 % with an average stimulus-lever-press latency of 2.64 ± 0.14 s. The response percentage decreased over time ($F(17,773)=3.92$, $P<1.9 \times 10^{-7}$, Fig. 1D), reflecting a change in motivation as rats accumulated sucrose rewards. However, this effect was not found in the response latency, which remained stable over time ($F(17,673)=0.69$, $P=0.836$, Fig. 1E).

Basic electrophysiological properties of Pf neurons

We recorded the activity of 399 Pf neurons (see Fig. 2 for histological reconstruction of the electrode sites). We first conducted analyses of neuronal responses to different task events: stimulus presentation, lever-pressing and reward collection. For this, we selected the attended trials in which the animals responded to the stimuli by lever-pressing and collected reward (Fig. 3).

We found that the majority of neurons were event-modulated, and of these neurons, more showed excitatory responses compared to inhibitory ones (254 and 88 neurons, respectively, $\chi^2=141$, $P<0.0001$). Excitations evoked by the stimulus occurred less frequently than those evoked by the lever-presses or the rewards (155, 229 and 228 neurons, respectively, $\chi^2=27.9.0$, $P<0.0001$, Fig. 3A). The different patterns of excitation/inhibition for different events were found in all seven recorded rats (Supplementary Table 1).

Across the population, we observed neurons with different waveform profiles and firing properties during the baseline period (i.e. 10 s preceding stimulus onset, Fig. 3B). The combination of responses to the different events was highly variable (Supplementary Table 2). As the number of neurons with opposite responses for different events was relatively low (49 out of 399, 12%), we decided to analyze separately the neurons excited and inhibited by

at least one task event. To account for rat variability, we included a subject-dependent factor in a two-way ANOVA test. Overall, event-excited neurons had lower baseline firing rate than event-inhibited neurons (9.81±0.78 vs. 15.27±1.63 Hz respectively; Response direction effect $F(1,371)=4.62$, $P=0.032$, Subject effect $F(4,371)=0.22$, $P=0.93$, Response direction x Subject $F(4,371)=0.19$, $P=0.94$, Fig. 3C). The other distributions were similar between excited and inhibited neurons (maximal frequency, 137.2±6.4 vs. 170.3±9.1 Hz respectively, Response direction effect $F(1,371)=1.81$, $P=0.18$, Subject effect $F(4,371)=3.97$, $P=0.004$, Response direction x Subject $F(4,371)=0.26$, $P=0.90$; spike width, 206±6 vs. 175±6 ms respectively, Response direction effect $F(1,371)=3.15$, $P=0.08$, Subject effect $F(4,371)=3.99$, $P=0.003$, Response direction x Subject $F(4,371)=0.68$, $P=0.61$, coefficient variation, 1.31±0.03 vs 1.36±0.05, Response direction effect $F(1,371)=0.51$, $P=0.47$, Subject effect $F(4,371)=5.06$, $P=0.0005$, Response direction x Subject $F(4,371)=0.79$, $P=0.53$, Fig. 3C-G). When these variables were plotted against each other, event-excited and inhibited neurons strongly overlapped and the two could not be separated based on these properties (Fig. 3E, H). We conducted similar analyses on excited and inhibited neurons separately for each event and obtained similar results (data not shown). Taken together, these results indicate that even if excited and inhibited neurons were to have different spiking properties, these differences were insufficient to separate the two populations.

Pf neuronal responses to task events

We then analyzed the temporal dynamics and magnitudes of these different event-evoked responses. While these neuronal responses often lasted several seconds, the behavioral events that evoked them, stimulus presentation, lever-pressing and reward collection occurred in close temporal proximity with much shorter latencies. PSTHs constructed around each of these events can potentially be distorted by the presence of other temporally correlated events. Thus, PSTHs do not allow one to accurately account for the neuronal responses to each individual event. To circumvent this issue, we used an iterative deconvolution method that takes advantage of the trial-to-trial variability in the temporal relationship between the different events to parse out the neuronal responses of each individual events from the PSTHs [34]. For each neuron, we deconvolved single-event responses by using the optimal number of iterations that achieved a cross-validation error

lower than the PSTHs (5.2 ± 0.2 iterations for the entire dataset). Figure 4A shows the rasters and PSTHs of an example neuron aligned to the three events. When the activity was lined up to stimulus presentation (left panel), the PSTH (gray line) showed a bimodal response, with the first activity peak related to the stimuli themselves and the second to lever-presses/rewards that occurred at different latencies on different trials (see raster). Deconvolution (brown line) reduced the contribution of the lever-press/reward-related activity while preserving the initial excitation to the stimulus. When aligned to lever-press, the raw PSTH shows a ramp followed by a sharp peak during the first second after the lever-press. Deconvolution suppressed the ramp that was mainly driven by the stimulus presentations but kept the peak response unaffected. Similarly, the peak preceding reward delivery (right panel) was largely reduced by deconvolution, indicating that this activity was driven by lever-presses rather than reward deliveries. Figure 4B shows the activity profile of another neuron. The inspection of the rasters shows that this neuron was inhibited before and after lever-press and excited at reward delivery. As in the previous example, deconvolution allowed us to isolate these event-related firing responses by removing the contribution of the adjacent events. Overall, deconvolution significantly reduced the number of responses per neuron ($\chi^2=44$, $P=1.4 \times 10^{-9}$, Figure 4C).

The analysis of raw PSTHs aligned to the stimulus revealed that excitatory responses occurred at a stereotypical latency (58 ± 4 ms, Fig. 5A, C, D) with variable durations (1.57 ± 0.17 s, Fig. 5A, C, E). The removal of the contribution of neighboring events by deconvolution had no effect on the onset latency distribution of stimulus-evoked excitations (KS=0.147, $P=0.09$, Fig. 5D) but strongly decreased their durations (KS=0.278, $P=3.4 \times 10^{-5}$, Fig. 5E).

On raw PSTHs, most lever-press-evoked excitations emerged before the occurrence of the event (-0.830 ± 0.05 s) and lasted up to 4 s (1.26 ± 0.11 s). Reward-evoked excitations occurred even earlier (-1.36 ± 0.04 s) and lasted in average 1.18 ± 0.10 s (Fig. 5A, C, D). Deconvolution significantly shifted lever-press- and reward-evoked excitations closer to the event (KS=0.226, $P=4.3 \times 10^{-5}$ and KS=0.382, $P=3.0 \times 10^{-13}$, respectively, Fig. 5D) and considerably shortened their durations (KS=0.25, $P=3.3 \times 10^{-6}$ and KS=0.26, $P=1.8 \times 10^{-6}$, respectively, Fig. 5E). The analysis of the magnitude of evoked responses (Fig. 5F) revealed a strong influence of the event considered (2-way Repeated Measures ANOVA, Event effect, $F(2,606)=123.6$, $P=9 \times 10^{-46}$) and the use of deconvolution (Deconvolution effect, $F(1,606)=355$, $P=1.1 \times 10^{-62}$) but no

significant interaction between them (Event x Deconvolution, $F(2,602)=2.34$, $P=0.097$). Stimuli-evoked excitations were ~ 3 times significantly larger than those evoked by lever-presses and rewards (Bonferroni test on Event effect, $P=2 \times 10^{-38}$ and $P=8 \times 10^{-39}$, respectively) but lever-press- and reward-evoked excitations did not differ from each other.

Inhibitions analyzed on raw PSTHs shared many similarities with excitations, but deconvolution had less effect, suggesting that these responses were more temporally associated with the behavioral events (Fig. 6). Stimulus-evoked inhibitory responses occurred after 85 ± 9 ms (non-significantly different from excitations, $KS=0.264$, $P=0.09$, Fig. 6A, B, D) and lasted 1.38 ± 0.63 s (significantly shorter than excitations, $KS=0.335$, $P=0.0014$, Fig. 6E). Deconvolution had no effect on these measures ($KS=0.175$, $P=0.85$ and $KS=0.25$, $P=0.44$, respectively, Fig. 6B-E).

Inhibitions to lever-presses and rewards preceded the events for most neurons (-0.56 ± 0.09 s and -0.82 ± 0.10 , respectively, Fig. 6A, C, D) and deconvolution had no effect ($KS=0.18$, $P=0.18$ and $KS=0.21$, $P=0.14$, respectively, Fig. 6B, C, D). We observed a strong trend toward a reduction of the duration of lever-press-evoked inhibitions by deconvolution ($KS=0.22$, $P=0.053$). The durations of reward-evoked inhibitions were reduced significantly ($KS=0.312$, $P=0.006$, Fig. 6E).

The magnitude of inhibitory responses (Fig. 6F) depended on the event considered (2-way Repeated Measures ANOVA, Event effect, $F(2,181)=12.44$, $P=8.688 \times 10^{-6}$) and the use of deconvolution (Deconvolution effect, $F(1,181)=21.72$, $P=6.09 \times 10^{-6}$) but we found no significant interaction between them (Event x Deconvolution, $F(2,181)=0.53$, $P=0.585$). Inhibitions to the stimulus were larger than those to the lever-presses and rewards (Bonferroni test on Event effect, $P=1.9 \times 10^{-5}$ and $P=1.3 \times 10^{-5}$, respectively) but lever-press and reward-evoked excitations did not differ from each other.

Together, these results indicate that Pf neurons respond strongly to reward-predictive stimuli but are also modulated in anticipation of lever-pressing and reward collection.

Modulation of stimulus-evoked responses by the motivational state.

Our data showed that Pf neurons are strongly activated by stimuli when the rats engage in reward-seeking. We then sought to decipher whether stimuli-evoked neuronal modulations depended on motivational state. We took advantage of the fact that long sessions produce

enough trials in which the rats engaged themselves in reward-seeking in response to the stimulus (attended trials) and those in which they did not (unattended trials, Fig. 7). Visual inspection of the data revealed very brisk excitations leading us to use a higher time resolution (2 ms) to construct PSTHs and a shorter response duration requirement to detect excitations (4 ms). Because of the short latency of these responses that most certainly preceded the initiation of locomotion in response to the stimulus [36], we analyzed neuronal activity on raw and not deconvolved PSTHs. We observed a first population of 62 neurons (15.5%) with higher phasic activations in response to attended compared to unattended stimuli (2.87 ± 0.37 and 0.99 ± 0.20 Hz, respectively, paired t-test, $t_{61}=7.09$, $p=1.63 \times 10^{-9}$, Fig. 7A, B). We named these neurons MOTIV+ because their activation to the stimulus reflects the animal's motivation to engage in the task. We also found a second population of 40 neurons (10 %) that displayed an opposite pattern: they were more excited by unattended compared to attended stimuli (MOTIV- neurons, 0.52 ± 0.13 and 1.75 ± 0.33 Hz, respectively, paired t-test, $t(39)=-4.89$, $P=1.77 \times 10^{-5}$, Fig. 7A, B). The remaining neurons did not respond differently to stimuli on attended and unattended trials and are not presented here.

The analysis of the response profile dynamics revealed that excited MOTIV- neurons were excited at a considerably shorter onset latency than MOTIV+ neurons (30.4 ± 3.6 ms and 44.2 ± 2.8 ms, respectively, $KS=0.394$, $P=9.81 \times 10^{-4}$, Fig. 7C). The excitations of excited MOTIV- neurons to unattended stimuli were also considerably shorter than those of excited MOTIV+ neurons to attended stimuli (117 ± 29 ms and 436 ± 87 ms, respectively, $KS=0.403$, $P=6.92 \times 10^{-4}$, Fig. 7C).

The analysis of the basic electrophysiological features of this population (Supplementary Figure 1) revealed that excited MOTIV+ neurons had a lower basal firing rate than excited MOTIV- neurons (8.59 ± 1.55 and 19.4 ± 3.27 Hz, respectively, $KS=0.36$, $P=0.002$) and a trend toward a longer spike width (223 ± 14 and 186 ± 10 ms, respectively, $KS=0.26$, $P=0.056$). We found no differences in the maximal frequency (146 ± 16 and 151 ± 15 Hz, respectively, $KS=0.22$, $P=0.15$) and the coefficient of variation (1.41 ± 0.07 and 1.34 ± 0.07 , respectively, $KS=0.18$, $P=0.34$).

Within the population of excited MOTIV+ neurons, 66% were also excited by lever-presses, a proportion that was higher than that of the entire population ($KS=11.77$, $P=0.003$,

Supplementary Figure 3). Reward excitations were under-represented ($KS=5.80$, $P=0.0055$). For excited MOTIV- neurons, the overall responses to lever-presses and rewards were small and did not differ in proportion compared to the entire population ($KS=2.56$, $P=0.28$ and $KS=5.43$, $P=0.07$, Supplementary Figure 4).

We conducted a similar analysis on stimuli-inhibited neurons on 20 ms-time-based PSTHs (Fig. 8) and found 21 MOTIV+ and 3 MOTIV- neurons. Inhibited MOTIV+ neurons were more inhibited to attended than unattended stimuli (2.44 ± 0.38 and 0.16 ± 0.41 Hz, respectively, paired t-test, $t(20)=-5.718$, $p=1.35\times 10^{-5}$). The onset latency to attended stimuli was 78 ± 11 ms and lasted 535 ± 132 ms. Given the low number of inhibited MOTIV- neurons, we did not analyze them further.

Inhibited MOTIV+ neurons had a high basal firing rate of 25.66 ± 4.3 Hz, a short spike width of 149 ± 9 ms, a maximal frequency of 167 ± 22 Hz and a coefficient of variation of 1.08 ± 0.12 (Supplementary Figure 2).

This population of neurons also had more inhibitory responses to the lever-press and the reward delivery than that found in the entire population ($KS=10.81$, $P=0.004$ and $KS=7.10$, $P=0.028$, supplementary Figure 5).

DISCUSSION

We sought to characterize the electrophysiological activity of Pf neurons in rats performing a stimulus-driven reward-seeking task. Most Pf neurons respond to different task events with a higher proportion of excitations than inhibitions. The waveforms and discharge properties were not predictive of their excited or inhibited responses to task events. Stimuli evoked larger responses than lever-pressing and rewards collection. The most striking finding was that excitations to stimuli depended on whether the animal subsequently engaged in reward-seeking.

Basic electrophysiological properties of Pf neurons

Pf neurons have traditionally been identified as a homogeneous population of glutamatergic neurons with long-range projections [23,37,38]. However, several studies have now revealed

Pf subtypes with distinct morphological and electrophysiological signatures. Neurons with bushy dendritic trees have higher maximal discharge rates and burstiness than neurons with diffuse branching dendrites [39,40]. Furthermore, a recent study found that in mice, the caudal Pf contains a small but significant proportions of GABA neurons that also have short action potential durations and high discharge rates [41]. Our analysis of the basic electrophysiologic features did reveal a strong dispersion in the parameters studied; they were strongly overlapping and we could not determine criteria to cluster different populations. We did find that inhibited neurons had significantly higher basal firing rates and shorter spike widths, suggesting that they could correspond to GABA and/or bushy neurons. However, further studies are required to test whether different subtypes can be identified with parameters sampled in extracellular recordings.

Pf neurons are activated during the behavioral approach

We found a very high prevalence of neurons modulated by task events with a strong bias toward excitations. Stimuli clearly evoked the strongest responses, for both excited and inhibited neurons. We speculate that this is related to the temporal unpredictability of stimuli presentations and their association with rewards that have both been shown to potentiate excitatory responses in primate CM/Pf [16,28]. We found that stimuli-evoked responses occurred at a relatively constant latency with large variations in their duration. In many cases, excitations persisted until the rat lever-pressed. The long sessions allowed animals to demonstrate differences in task engagement. These differences were associated with large variability in the response latency within and between sessions, which likely explained the variability in the durations of excitations. Deconvolution allowed us to isolate neuronal activity time-locked to particular behavioral events by removing the contribution of neighboring events [34,35]. The fact that deconvolution shortened stimulus- and action-evoked excitations suggests that the behavioral approach by itself activated Pf neurons. Interestingly, such pattern of anticipatory activity seems to be found in both primates and mice [19,31]. In a task where monkeys had to perform specific actions in response to instructive stimuli, long-latency facilitation (LLF) neurons recorded in CM displayed a biphasic response with inhibition followed by excitation to stimuli. The latter appeared more strongly correlated with the timing of the required action than the instructive stimulus directing it [31]. Furthermore, a local inactivation of the CM with the GABA agonist muscimol decreased the number of licks

in a pavlovian task [16], indicating that LLF activity contributes to behavioral responding. In mice performing a fixed-ratio 8 schedule task in which no explicit stimuli were presented, Pf neurons also displayed excitation that preceded the first lever-press and that was shown to be necessary for task performance. Indeed, an optogenetic inhibition of striatum-projecting Pf neurons increased the latency to re-engage in a trial without affecting the repeated motor sequence of lever-pressing [19]. Altogether, these results indicate that the excitation of Pf neurons during the behavioral approach is causal.

Amongst stimulus-inhibited neurons, a few (5 out of 399) displayed the characteristic biphasic inhibition-excitation found in LLF neurons revealing a similarity with the primate CM. Inhibitions evoked by instrumental actions, often associated with preceding excitations are also found in mice [19]. But overall, inhibitory responses were considerably less frequent than excitation. Thus, exploring their role will require further studies manipulating specifically these populations.

Influence of the motivational state on Pf responses to incentive stimuli

In primates, CM neurons respond to unconditioned auditory and visual stimulations [16]. The amplitude of these responses decreased as the stimuli became predictive of rewards indicating that conditioning induced a form of long-term plasticity. However, whether Pf neuronal responses could be rapidly modulated was unknown. The use of long sessions allowed us to analyze Pf neuronal activity in response to stimuli predicting the same rewards while rats were in different motivational states. We compared the trials to which the animal attended to the stimulus by engaging in behavioral response (and thus obtaining the reward) and those they did not. The absence of engagement on unattended trials was unlikely due to a failure in perceiving the stimulus that was highly salient and long lasting (300 ms-long 85 dB white noise coupled to the visual extension of the lever for 10 s). The strongest evidence against this hypothesis is the fact that we identified a population of neurons that was more excited to the stimulus on unattended trials, indicative of an active process taking place in these situations. Most likely, the absence of responding was caused by the fact that at certain times, animals in these long sessions valued reward-seeking less than other activities (e.g. grooming, exploring, resting).

MOTIV+ neurons exhibited either excitation or inhibition to attended stimuli in the first 100 ms of their presentations. In a similar task, locomotion onset has been reported to start ~250

ms after a reward-predictive stimulus, indicating that the initial component of the responses of MOTIV+ neurons was not driven by movements themselves [36] but could instead participate in initiating them. It seems unlikely that excited MOTIV+ neurons are the homolog to primate LLF neurons for two reasons. First, inhibition precedes the excitation in LLF neurons [16]. Second, the amplitude of the excitatory component of LLF neurons is inversely correlated with the reaction time on a trial-to-trial basis [31]. The stronger response to attended stimuli compared to unattended stimuli in the present study is diametrically opposed to this observation. Thus, the excited MOTIV+ profile reported in this study does not seem to match LLF activity reported in primates. However, we did find, among inhibited MOTIV+ neurons, some profiles that matched primate LLF neurons. Both excited and inhibited MOTIV+ neurons could participate in action engagement in response to the stimulus. Testing this hypothesis will require tools to selectively manipulate these populations.

Excited MOTIV- neurons had stereotyped responses with excitations starting as early as 6 ms after stimulus onset and lasting less than 100 ms. Yet, these brisk responses were associated with the absence of behavioral responding in the next 10 s. These data provide further evidence that the Pf carries an important attentional function [10,24,28,42] by gathering low level sensory information that may arise from the deep layers of the superior colliculi and/or the pedunculopontine nucleus [43–45]. Excited MOTIV- neurons shared properties with short-latency facilitation neurons (SLF) recorded in the primate CM [16]. But importantly, the early and transient firing of excited MOTIV- neurons, manifested when the rat did not attend to stimuli, indicates that their attention was not directed toward them. To the contrary, CM recordings and inactivations in monkeys during a countermanding task provided evidence that SLF neurons participate in the direction of attention toward stimuli [28]. This apparent discrepancy could relate to the modality used in these studies (auditory and visual in our study and purely visual in the primate study) or even different functions carried by Pf neurons in different species. Another intriguing possibility lies in the characteristics of the stimuli used. Minamimoto and Kimura (2002) presented temporally predictable stimuli that provided instructions to the monkeys about the direction of the saccade to be rewarded. In our study, we used stimuli that were presented unexpectedly and incentivized the rats to switch from their current activity to reward-seeking by engaging in actions during a 10 s-time window. These actions strongly differed depending on the location of the rats at the time of occurrence

of these stimuli. Thus, the Pf could subserve different roles for instructive and incentive stimuli as we previously showed for NAc neurons [33].

The excitations of MOTIV- neurons could block processes that facilitate task engagement through the dense Pf projection to the striatal complex [5]. As opposed to other thalamic nuclei, the Pf preferentially synapses on cholinergic interneurons (CINs) [14,46–48] that exert a strong inhibitory control on the activity of medium spiny projection neurons (MSNs) *in vivo* [49] through different GABA interneuron subtypes [13,50,51]. We recently reported that NAc Core CINs were also more active in response to unattended than attended incentive stimuli [33]. The short latencies observed in CINs suggest that they could be driven by excited MOTIV-Pf neurons.

Excitations of NAc MSNs evoked by incentive stimuli are necessary for rats to engage in action [35] and depend on ventral tegmental area [52], basolateral amygdala [53] and paraventricular [20] inputs. The present work indicates that the Pf projection to NAc could subserve an opposite role by repressing behavioral responding. Further work is needed to directly test this hypothesis.

CONTRIBUTIONS

MS conducted experiments, analyzed data, prepared figures and wrote the initial draft of the manuscript. JM designed research, supervised MS, participated to experiments and edited the manuscript. FA designed research, analyzed data, prepared figures and edited the manuscript.

FUNDING

This work was supported by the ATIP/Avenir Program, the Centre National de la Recherche Scientifique (CNRS) and Aix-Marseille Université (AMU).

ACKNOWLEDGEMENTS

The authors thank Didier Louber and Dany Paleressompouille for technical support and Louis Kang for proof reading this manuscript.

DECLARATION OF INTEREST

The authors declare no conflict of interest.

REFERENCES

- [1] Ariens-Kappers, C.; Huber, G.; Crosby, E. *The Comparative Anatomy of the Nervous System of Vertebrates, Including Man*; Macmillan, Ed.; New York, NY, 1936.
- [2] Butler, A. B. The Evolution of the Dorsal Thalamus of Jawed Vertebrates, Including Mammals: Cladistic Analysis and a New Hypothesis. *Brain Research Reviews*. 1994, pp 29–65.
- [3] James, M. H.; Charnley, J. L.; Levi, E. M.; Jones, E.; Yeoh, J. W.; Smith, D. W.; Dayas, C. V. Orexin-1 Receptor Signalling within the Ventral Tegmental Area, but Not the Paraventricular Thalamus, Is Critical to Regulating Cue-Induced Reinstatement of Cocaine-Seeking. *Int. J. Neuropsychopharmacol.* **2011**, *14* (5), 684–690.
- [4] Rikhye, R. V.; Wimmer, R. D.; Halassa, M. M. Toward an Integrative Theory of Thalamic Function. *Annu. Rev. Neurosci* **2018**, *41*, 163–183.
- [5] Van Der Werf, Y. D.; Witter, M. P.; Groenewegen, H. J. The Intralaminar and Midline Nuclei of the Thalamus. Anatomical and Functional Evidence for Participation in Processes of Arousal and Awareness. *Brain Res. Rev.* **2002**, *39* (2–3), 107–140.
- [6] Redgrave, P.; Prescott, T. J.; Gurney, K. The Basal Ganglia: A Vertebrate Solution to the Selection Problem? *Neuroscience*. 1999, pp 1009–1023.
- [7] Hikosaka, O.; Kim, H. F.; Yasuda, M.; Yamamoto, S. Basal Ganglia Circuits for Reward Value-Guided Behavior. *Annu. Rev. Neurosci.* **2014**, *37* (1), 289–306.
- [8] Alexander, G. Parallel Organization of Functionally Segregated Circuits Linking Basal Ganglia and Cortex. *Annu. Rev. Neurosci.* **1986**, *9* (1), 357–381.

- [9] McHaffie, J. G.; Stanford, T. R.; Stein, B. E.; Coizet, V.; Redgrave, P. Subcortical Loops through the Basal Ganglia. *Trends Neurosci.* **2005**, *28* (8), 401–407.
- [10] Redgrave, P.; Vautrelle, N.; Reynolds, J. N. J. Functional Properties of the Basal Ganglia's Re-Entrant Loop Architecture: Selection and Reinforcement. *Neuroscience* **2011**, *198*, 138–151.
- [11] Redgrave, P.; Gurney, K. The Short-Latency Dopamine Signal: A Role in Discovering Novel Actions? *Nat. Rev. Neurosci.* **2006**, *7* (12), 967–975.
- [12] Ding, J. B.; Guzman, J. N.; Peterson, J. D.; Goldberg, J. a; Surmeier, D. J. Thalamic Gating of Corticostriatal Signaling by Cholinergic Interneurons. *Neuron* **2010**, *67* (2), 294–307.
- [13] English, D. F.; Ibanez-Sandoval, O.; Stark, E.; Tecuapetla, F.; Buzsáki, G.; Deisseroth, K.; Tepper, J. M.; Koos, T. GABAergic Circuits Mediate the Reinforcement-Related Signals of Striatal Cholinergic Interneurons. *Nat. Neurosci.* **2012**, *15* (1), 123–130.
- [14] Doig, N. M.; Magill, P. J.; Apicella, P.; Bolam, J. P.; Sharott, A. Cortical and Thalamic Excitation Mediate the Multiphasic Responses of Striatal Cholinergic Interneurons to Motivationally Salient Stimuli. *J. Neurosci.* **2014**, *34* (8), 3101–3117.
- [15] Mandelbaum, G.; Taranda, J.; Haynes, T. M.; Hochbaum, D. R.; Huang, K. W.; Hyun, M.; Umadevi Venkataraju, K.; Straub, C.; Wang, W.; Robertson, K.; Osten, P.; Sabatini, B. L. Distinct Cortical-Thalamic-Striatal Circuits through the Parafascicular Nucleus. *Neuron* **2019**, *102* (3), 636-652.e7.
- [16] Matsumoto, N.; Minamimoto, T.; Graybiel, A. M.; Kimura, M. Neurons in the Thalamic CM-Pf Complex Supply Striatal Neurons with Information about Behaviorally Significant Sensory Events. *J. Neurophysiol.* **2001**, *85* (2), 960–976.
- [17] Bradfield, L. A.; Bertran-Gonzalez, J.; Chieng, B.; Balleine, B. W. The Thalamostriatal Pathway and Cholinergic Control of Goal-Directed Action: Interlacing New with Existing

- Learning in the Striatum. *Neuron* **2013**, *79* (1), 153–166.
- [18] Do-Monte, F. H.; Minier-Toribio, A.; Quiñones-Laracuate, K.; Medina-Colón, E. M.; Quirk, G. J. Thalamic Regulation of Sucrose Seeking during Unexpected Reward Omission. *Neuron* **2017**, *94* (2), 388-400.e4.
- [19] Díaz-Hernández, E.; Contreras-López, R.; Sánchez-Fuentes, A.; Rodríguez-Sibrían, L.; Ramírez-Jarquín, J. O.; Tecuapetla, F. The Thalamostriatal Projections Contribute to the Initiation and Execution of a Sequence of Movements. *Neuron* **2018**, *100* (3), 739-752.e5.
- [20] Meffre, J.; Sicre, M.; Diarra, M.; Marchessaux, F.; Paleressompoulle, D.; Ambroggi, F. Orexin in the Posterior Paraventricular Thalamus Mediates Hunger-Related Signals in the Nucleus Accumbens Core. *Curr. Biol.* **2019**, *29* (19), 3298-3306.e4.
- [21] Hamlin, A. S.; Clemens, K. J.; Choi, E. a; McNally, G. P. Paraventricular Thalamus Mediates Context-Induced Reinstatement (Renewal) of Extinguished Reward Seeking. *Eur. J. Neurosci.* **2009**, *29* (4), 802–812.
- [22] Jones, E. G.; Leavitt, R. Y. Retrograde Axonal Transport and the Demonstration of Non-specific Projections to the Cerebral Cortex and Striatum from Thalamic Intralaminar Nuclei in the Rat, Cat and Monkey. *J. Comp. Neurol.* **1974**, *154* (4), 349–377.
- [23] Smith, Y.; Raju, D. V; Pare, J.-F.; Sidibe, M. The Thalamostriatal System: A Highly Specific Network of the Basal Ganglia Circuitry. *Trends Neurosci.* **2004**, *27* (9), 520–527.
- [24] Smith, Y.; Surmeier, D. J.; Redgrave, P.; Kimura, M. Thalamic Contributions to Basal Ganglia-Related Behavioral Switching and Reinforcement. *J. Neurosci.* **2011**, *31* (45), 16102–16106.
- [25] Berendse, H. W.; Groenewegen, H. J. Organization of the Thalamostriatal Projections in the Rat, with Special Emphasis on the Ventral Striatum. *J. Comp. Neurol.* **1990**, *299* (2),

- 187–228.
- [26] Berendse, H. W.; Groenewegen, H. J. Restricted Cortical Termination Fields of the Midline and Intralaminar Thalamic Nuclei in the Rat. *Neuroscience* **1991**, *42* (1), 73–102.
- [27] Groenewegen, H. J.; Berendse, H. W. The Specificity of the “nonspecific” Midline and Intralaminar Thalamic Nuclei. *Trends in Neurosciences*. Trends Neurosci 1994, pp 52–57.
- [28] Minamimoto, T.; Kimura, M. Participation of the Thalamic CM-Pf Complex in Attentional Orienting. *J. Neurophysiol.* **2002**, *87* (6), 3090–3101.
- [29] Kimura, M.; Minamimoto, T.; Matsumoto, N.; Hori, Y. Monitoring and Switching of Cortico-Basal Ganglia Loop Functions by the Thalamo-Striatal System. *Neurosci. Res.* **2004**, *48* (4), 355–360.
- [30] Minamimoto, T.; Hori, Y.; Kimura, M. Neuroscience: Complementary Process to Response Bias in the Centromedian Nucleus of the Thalamus. *Science (80-.)*. **2005**, *308* (5729), 1798–1801.
- [31] Minamimoto, T.; Hori, Y.; Yamanaka, K.; Kimura, M. Neural Signal for Counteracting Pre-Action Bias in the Centromedian Thalamic Nucleus. *Front. Syst. Neurosci.* **2014**, *8* (JAN).
- [32] du Hoffmann, J.; Kim, J. J.; Nicola, S. M. An Inexpensive Drivable Cannulated Microelectrode Array for Simultaneous Unit Recording and Drug Infusion in the Same Brain Nucleus of Behaving Rats. *J. Neurophysiol.* **2011**, *106* (2), 1054–1064.
- [33] Sicre, M.; Meffre, J.; Louber, D.; Ambroggi, F. The Nucleus Accumbens Core Is Necessary for Responding to Incentive but Not Instructive Stimuli. *J. Neurosci.* **2020**, *40* (6), 1332–1343.
- [34] Ghazizadeh, A.; Fields, H. L.; Ambroggi, F. Isolating Event-Related Neuronal Responses by Deconvolution. *J. Neurophysiol.* **2010**, *104* (3), 1790–1802.

- [35] Ambroggi, F.; Ghazizadeh, A.; Nicola, S. M.; Fields, H. L. Roles of Nucleus Accumbens Core and Shell in Incentive-Cue Responding and Behavioral Inhibition. *J. Neurosci.* **2011**, *31* (18), 6820–6830.
- [36] McGinty, V. B.; Lardeux, S.; Taha, S. A.; Kim, J. J.; Nicola, S. M. Invigoration of Reward Seeking by Cue and Proximity Encoding in the Nucleus Accumbens. *Neuron* **2013**, *78* (5), 910–922.
- [37] Wilson, C. J.; Chang, H. T.; Kitai, S. T. Origins of Post Synaptic Potentials Evoked in Spiny Neostriatal Projection Neurons by Thalamic Stimulation in the Rat. *Exp. Brain Res.* **1983**, *51* (2), 217–226.
- [38] Mouroux, M.; Féger, J. Evidence That the Parafascicular Projection to the Subthalamic Nucleus Is Glutamatergic. *Neuroreport* **1993**, *4* (6), 613–615.
- [39] Beatty, J. A.; Sylwestrak, E. L.; Cox, C. L. Two Distinct Populations of Projection Neurons in the Rat Lateral Parafascicular Thalamic Nucleus and Their Cholinergic Responsiveness. *Neuroscience* **2009**, *162* (1), 155–173.
- [40] Mendez-Rodriguez, B. S.; Arias-Garcia, M. A.; Tapia, D.; Laville, A.; Bargas, J.; Galarraga, E. Firing Differences Between Adult Intralaminar Thalamo-Striatal Neurons. *Neuroscience* **2021**.
- [41] Chen, B.; Xu, C.; Wang, Y.; Lin, W.; Wang, Y.; Chen, L.; Cheng, H.; Xu, L.; Hu, T.; Zhao, J.; Dong, P.; Guo, Y.; Zhang, S.; Wang, S.; Zhou, Y.; Hu, W.; Duan, S.; Chen, Z. A Disinhibitory Nigra-Parafascicular Pathway Amplifies Seizure in Temporal Lobe Epilepsy. *Nat. Commun.* **2020**, *11* (1).
- [42] Minamimoto, T.; Hori, Y.; Kimura, M. Roles of the Thalamic CM-PF Complex-Basal Ganglia Circuit in Externally Driven Rebias of Action. *Brain Research Bulletin.* 2009, pp 75–79.

- [43] Krout, K. E.; Loewy, a D.; Westby, G. W.; Redgrave, P. Superior Colliculus Projections to Midline and Intralaminar Thalamic Nuclei of the Rat. *J. Comp. Neurol.* **2001**, *431* (2), 198–216.
- [44] Krauthamer, G. M.; Krol, J. G.; Grunweg, B. S. Effect of Superior Colliculus Lesions on Sensory Unit Responses in the Intralaminar Thalamus of the Rat. *Brain Res.* **1992**, *576* (2), 277–286.
- [45] Paré, D.; Smith, Y.; Parent, A.; Steriade, M. Projections of Brainstem Core Cholinergic and Non-Cholinergic Neurons of Cat to Intralaminar and Reticular Thalamic Nuclei. *Neuroscience* **1988**, *25* (1), 69–86.
- [46] Sidibé, M.; Smith, Y. Thalamic Inputs to Striatal Interneurons in Monkeys: Synaptic Organization and Co-Localization of Calcium Binding Proteins. *Neuroscience* **1999**, *89* (4), 1189–1208.
- [47] Lapper, S. R.; Bolam, J. P. Input from the Frontal Cortex and the Parafascicular Nucleus to Cholinergic Interneurons in the Dorsal Striatum of the Rat. *Neuroscience* **1992**, *51* (3), 533–545.
- [48] Raju, D. V; Shah, D. J.; Wright, T. M.; Hall, R. a; Smith, Y. Differential Synaptology of VGluT2-Containing Thalamostriatal Afferents between the Patch and Matrix Compartments in Rats. *J. Comp. Neurol.* **2006**, *499* (2), 231–243.
- [49] Witten, I. B.; Lin, S. C.; Brodsky, M.; Prakash, R.; Diester, I.; Anikeeva, P.; Gradinaru, V.; Ramakrishnan, C.; Deisseroth, K. Cholinergic Interneurons Control Local Circuit Activity and Cocaine Conditioning. *Science (80-.)*. **2010**, *330* (6011), 1677–1681.
- [50] Assous, M.; Kaminer, J.; Shah, F.; Garg, A.; Ko?s, T.; Tepper, J. M. Differential Processing of Thalamic Information via Distinct Striatal Interneuron Circuits. *Nat. Commun.* **2017**, *8* (May), 15860.

- [51] Assous, M.; Tepper, J. M. Excitatory Extrinsic Afferents to Striatal Interneurons and Interactions with Striatal Microcircuitry. *European Journal of Neuroscience*. Wiley/Blackwell (10.1111) March 25, 2018.
- [52] Yun, I. A.; Wakabayashi Ken T.; Fields, H. L.; Nicola, S. M. The Ventral Tegmental Area Is Required for the Behavioral and Nucleus Accumbens Neuronal Firing Responses to Incentive Cues. *J. Neurosci.* **2004**, *24* (12), 2923–2933.
- [53] Ambroggi, F.; Ishikawa, A.; Fields, H. L.; Nicola, S. M. Basolateral Amygdala Neurons Facilitate Reward-Seeking Behavior by Exciting Nucleus Accumbens Neurons. *Neuron* **2008**, *59* (4), 648–661.

FIGURE LEGENDS

Fig.1. Behavioral performance in the stimulus-driven reward seeking task.

A. Task diagram showing the sequence of events. **B.** Temporal structure of the task. **C.** Individual percentage of responses and latencies for all sessions (n=46). Animals (n=7) are color-coded. Histograms represent the distributions of the percent responses (yellow) and latencies (purple). **D.** Top: Heatmaps representing the percentage of responses to the stimulus over time. Each line corresponds to a single session. Data are grouped per animals (labeled with the right color bar). Bottom: average percent responding as mean+/-sem. **E.** Same representation than in D for behavioral latencies.

Fig.2. Histology and electrode path reconstruction.

A. Schematic diagram of a rat brain coronal section and representative photomicrograph of two electrode bundle tracks located in the Pf. **B.** Histological reconstruction of the recording sites in the Pf. Boxes represent the approximate extent of the electrode bundles in the 7 animals (color coded). Dotted line corresponds to the depth of the recording sessions.

Fig.3. Electrophysiological characteristics of Pf neurons excited and inhibited by the different task events.

A. Percentage of neurons excited (*left*) and inhibited (*right*) by the different events (stimulus, lever-press, reward). **B.** Example of three representative waveforms recorded in the Pf with their baseline firing rate. **C.** Cumulative percentage of baseline firing rate of task-excited (blue) and task-inhibited (red) neurons. **D.** Cumulative percentage of spike widths. **E.** Baseline firing rate plotted against spike width for individual neurons (gray dots indicate non-responsive neurons). **F.** Cumulative percentage of maximal frequencies. **G.** Cumulative percentage of the coefficients of variation. **H.** Coefficient of variations plotted against the maximal frequencies for individual neurons. *P<0.05

Fig.4. Deconvolution

A. Activity of an example neuron aligned to the stimulus (*left*), lever press (*middle*) and reward delivery (*right*). Top: raster plot with trials sorted by the latency to lever-press. Each gray line is an action potential. Brown squares represent stimuli presentations, orange squares, the lever-presses and blue squares, the reward deliveries. Bottom: gray lines represent the raw PSTH showing the average firing rate. Colored lines represent the deconvolved PSTH. **B.** Same representation for another example neuron. **C.** Venn diagrams showing the proportion of neurons excited (*left*) and inhibited (*right*) by task events using raw (top) or deconvolved (bottom) data.

Fig.5. Pf neuronal excitations to task events.

A. Heatmaps represent color-coded PSTHs showing neurons excited to the stimulus (*left*), lever-press (*middle*) and reward delivery (*right*). Each row represents the PSTH of an individual neuron aligned to the event considered. Data are plotted with smoothed 20 ms-time-bins and neurons are sorted by excitation durations for stimuli responses and onset latencies for lever-press and reward responses. **B.** Heatmaps represent deconvolved PSTHs of the same neurons represented in A. **C.** Average responses for the neurons shown in A and B. The gray traces correspond to raw PSTHs. Brown, orange and blue traces correspond to the deconvolved PSTHs to the stimulus, lever-press and reward delivery, respectively. **D.** Cumulative percentage of excitation onset latencies for raw and deconvolved responses. **E.** Cumulative percentage of excitations durations. **F.** Violin plots of the event-evoked firings. White dots indicate the median, black bars indicate the 25th and 75th percentiles of the distribution. The gray envelope is a rotated kernel density plot and colored dots show the individual values.

Fig.6. Pf neuronal inhibitions to task events.

A. Heatmaps represent color-coded PSTHs showing neurons inhibited to the stimulus (*left*), lever-press (*middle*) and reward delivery (*right*). Each row represents the PSTH of an individual neuron aligned to the event considered. Data are plotted with smoothed 20 ms-time-bins and neurons are sorted by inhibition durations for stimuli responses and onset latencies for lever-press and reward responses. **B.** Heat-maps represent deconvolved PSTH of the same neurons represented in A. **C.** Average responses for the neurons shown in A and B. The gray traces correspond to raw PSTHs. Brown, orange and blue traces correspond to the deconvolved PSTHs to the stimulus, lever-press and reward delivery, respectively. **D.** Cumulative percentage of inhibition onset latencies for raw and deconvolved responses. **E.** Cumulative percentage of inhibition durations. **F.** Violin plots of the event-evoked firings. White dots indicate the median, black bars indicate the 25th and 75th percentiles of the distribution. Gray envelope is a rotated kernel density plot and colored dots show individual values.

Fig.7. Pf neuronal excitations to the stimulus depend on whether the animal engages in reward-seeking.

A. Heatmaps showing stimuli-evoked excitations of neurons on trials the animals engaged in reward-seeking (*top*) and those they did not (*bottom*) for MOTIV+ (*left*) and MOTIV- (*right*) neurons. Neurons are sorted by onset latencies. Raw PSTHs are plotted with 2 ms-time-bins. **B.** Average PSTHs for excited MOTIV + and excited MOTIV- neurons for attended (brown) and unattended (gray) stimuli. **C.** Cumulative percentage of excitation latencies (*left*) and durations (*right*) for excited MOTIV+ (green) and excited MOTIV- (purple) neurons.

Fig.8. Pf neuronal inhibitions to the stimulus depends on whether the animal engages in reward-seeking.

A. Heatmaps showing stimuli-evoked inhibitions of neurons on trials the animals engaged in reward-seeking (*top*) and those they did not (*bottom*) for MOTIV+ (*left*) and MOTIV- (*right*) neurons. Neurons are sorted by onset latencies. Raw PSTHs are plotted with 20 ms-time-bins. **B.** Average PSTHs for inhibited MOTIV + and inhibited MOTIV- neurons for attended (brown) and unattended (gray) stimuli.

Supplementary Fig.1. Electrophysiological characteristics of excited MOTIV+ and MOTIV- neurons.

A. Cumulative percentage of baseline firing rate of excited MOTIV+ (green) and excited MOTIV- (purple) neurons. **B.** Cumulative percentage of spike widths. **C.** Baseline firing rate plotted against spike width for individual neurons. **D.** Cumulative percentage of maximal frequencies. **E.** Cumulative percentage of the coefficients of variation. **H.** Coefficient of variations plotted against the maximal frequencies for individual neurons.

Supplementary Fig.2. Electrophysiological characteristics of inhibited MOTIV+ and MOTIV- neurons.

A. Cumulative percentage of baseline firing rate of inhibited MOTIV+ (green) and inhibited MOTIV- (purple) neurons. **B.** Cumulative percentage of spike widths. **C.** Baseline firing rate plotted against spike width for individual neurons. **D.** Cumulative percentage of maximal frequencies. **E.** Cumulative percentage of the coefficients of variation. **H.** Coefficient of variations plotted against the maximal frequencies for individual neurons.

Supplementary Fig.3. Neuronal responses of excited MOTIV+ neurons to lever-presses and reward deliveries. **A.** Proportion of excited, inhibited and non-responsive neurons for lever-presses (*left*) and reward deliveries (*right*). The internal pie charts represent the proportions of responses in the entire data set (n=399). The ring charts represent the same proportions for the population of excited MOTIV+

neurons. B. Heatmaps (top) and PSTHs (bottom). C. Violin plots of lever-press- and reward delivery-evoked firing.

Supplementary Fig.4. Neuronal responses of excited MOTIV- neurons to lever-presses and reward deliveries. A. Proportion of excited, inhibited and non-responsive neurons for lever-presses (left) and reward deliveries (right). The internal pie charts represent the proportions of responses in the entire data set (n=399). The ring charts represent the same proportions for the population of excited MOTIV- neurons. B. Heatmaps (top) and PSTHs (bottom). C. Violin plots of lever-press- and reward delivery-evoked firing.

Supplementary Fig.5. Neuronal responses of inhibited MOTIV+ neurons to lever-presses and reward deliveries. A. Proportion of excited, inhibited and non-responsive neurons for lever-presses (left) and reward deliveries (right). The internal pie charts represent the proportions of responses in the entire data set (n=399). The ring charts represent the same proportions for the population of inhibited MOTIV+ neurons. B. Heatmaps (top) and PSTHs (bottom). C. Violin plots of lever-press- and reward delivery-evoked firing.

FIGURES

Figure 1

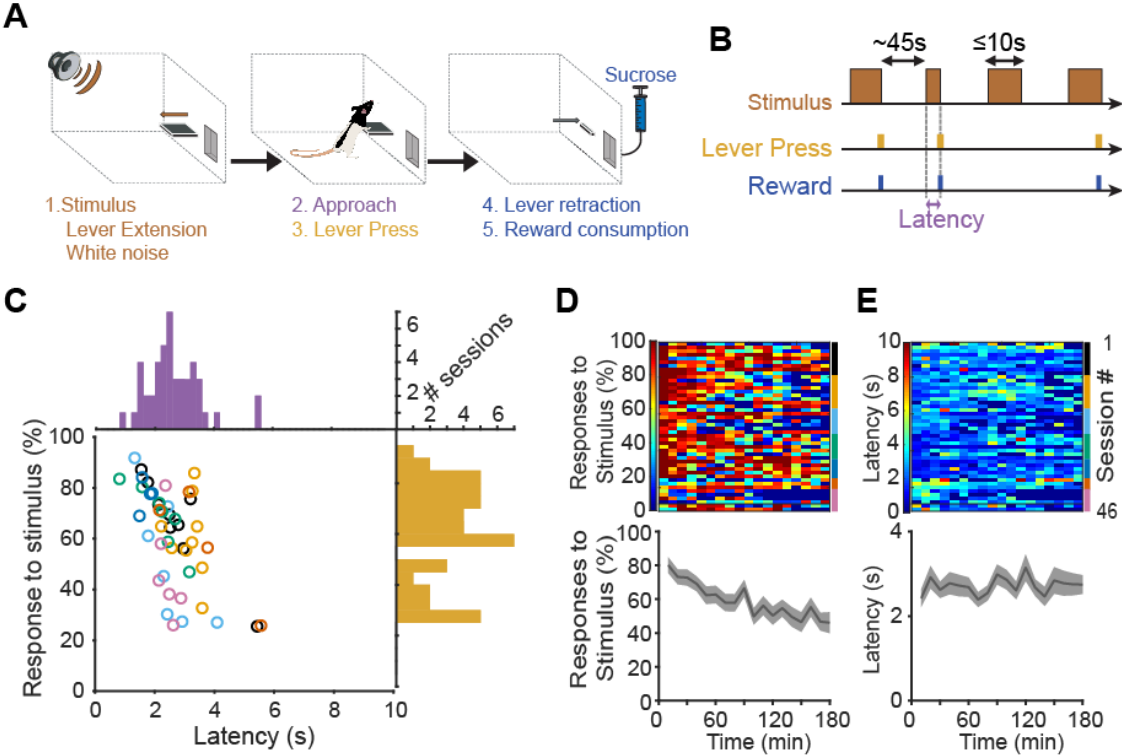


Figure 2

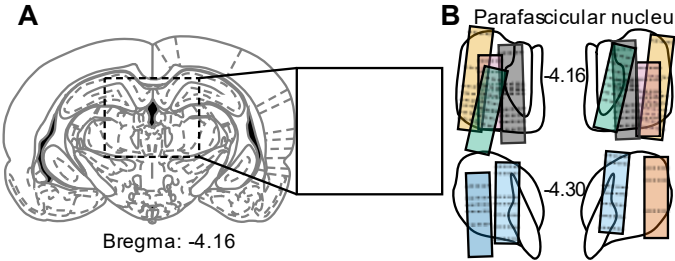


Figure 3

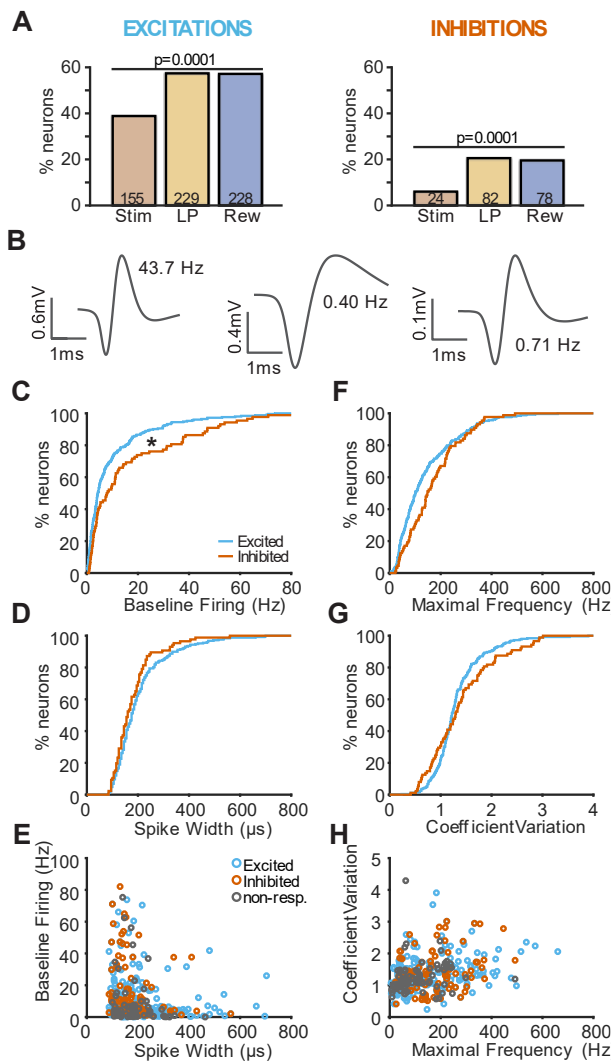


Figure 4

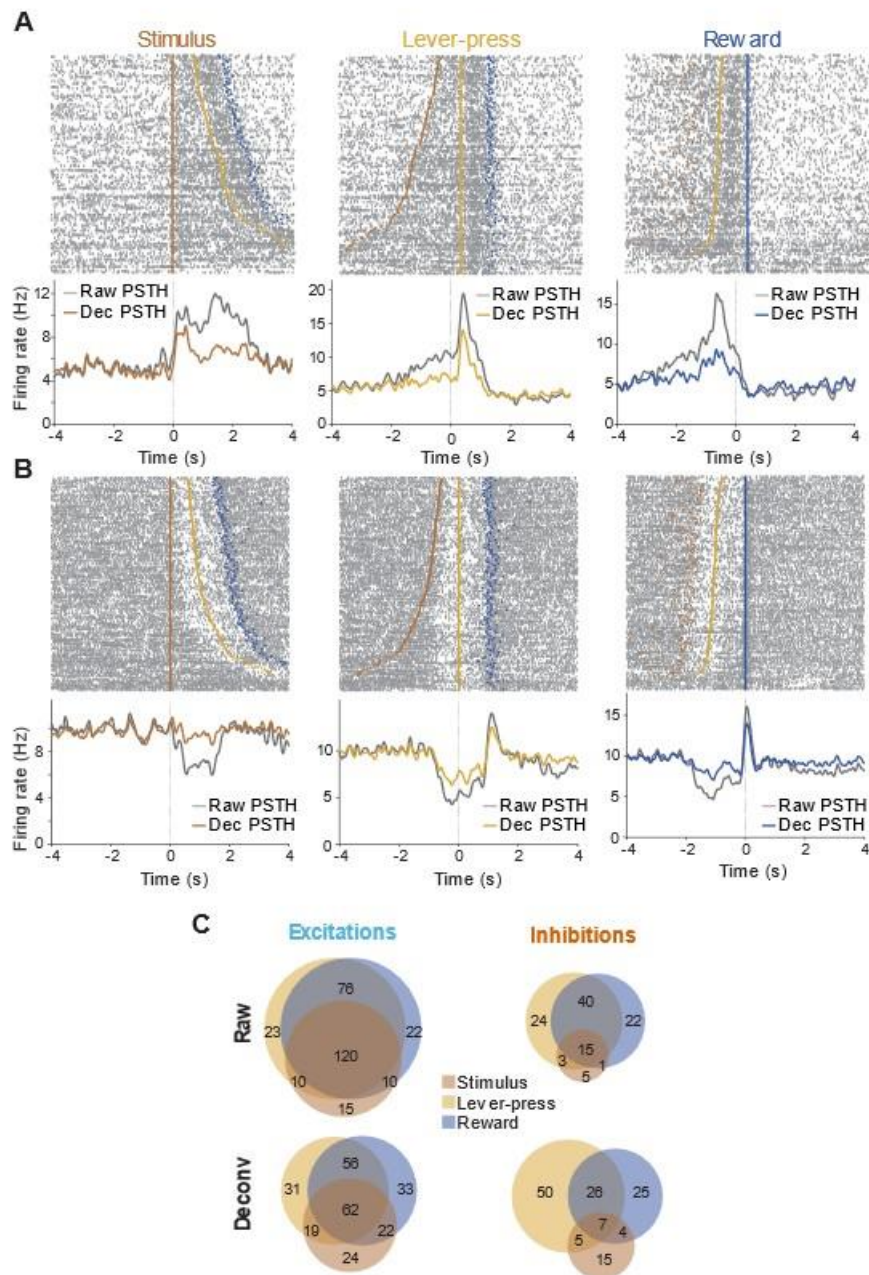


Figure 5

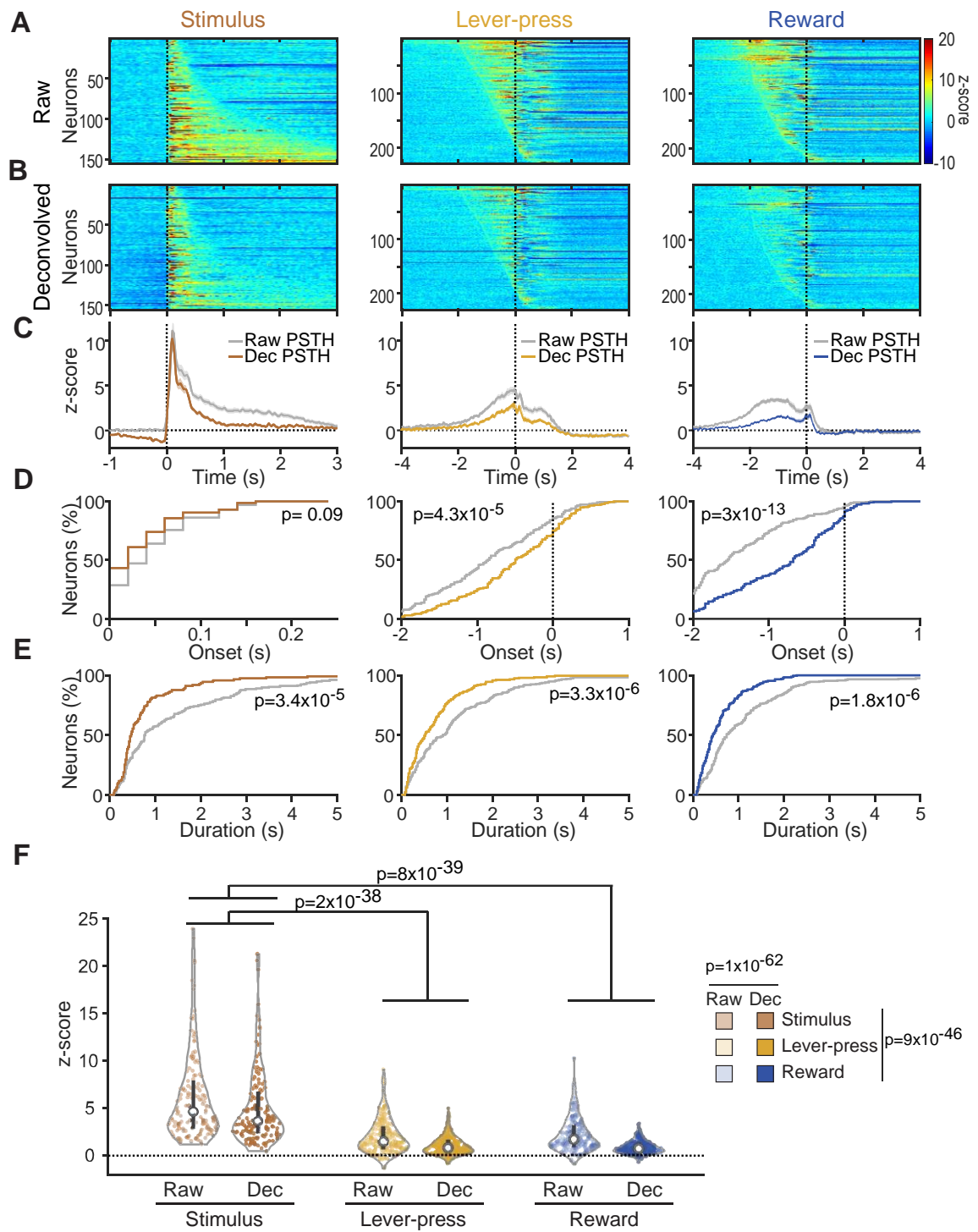


Figure 6

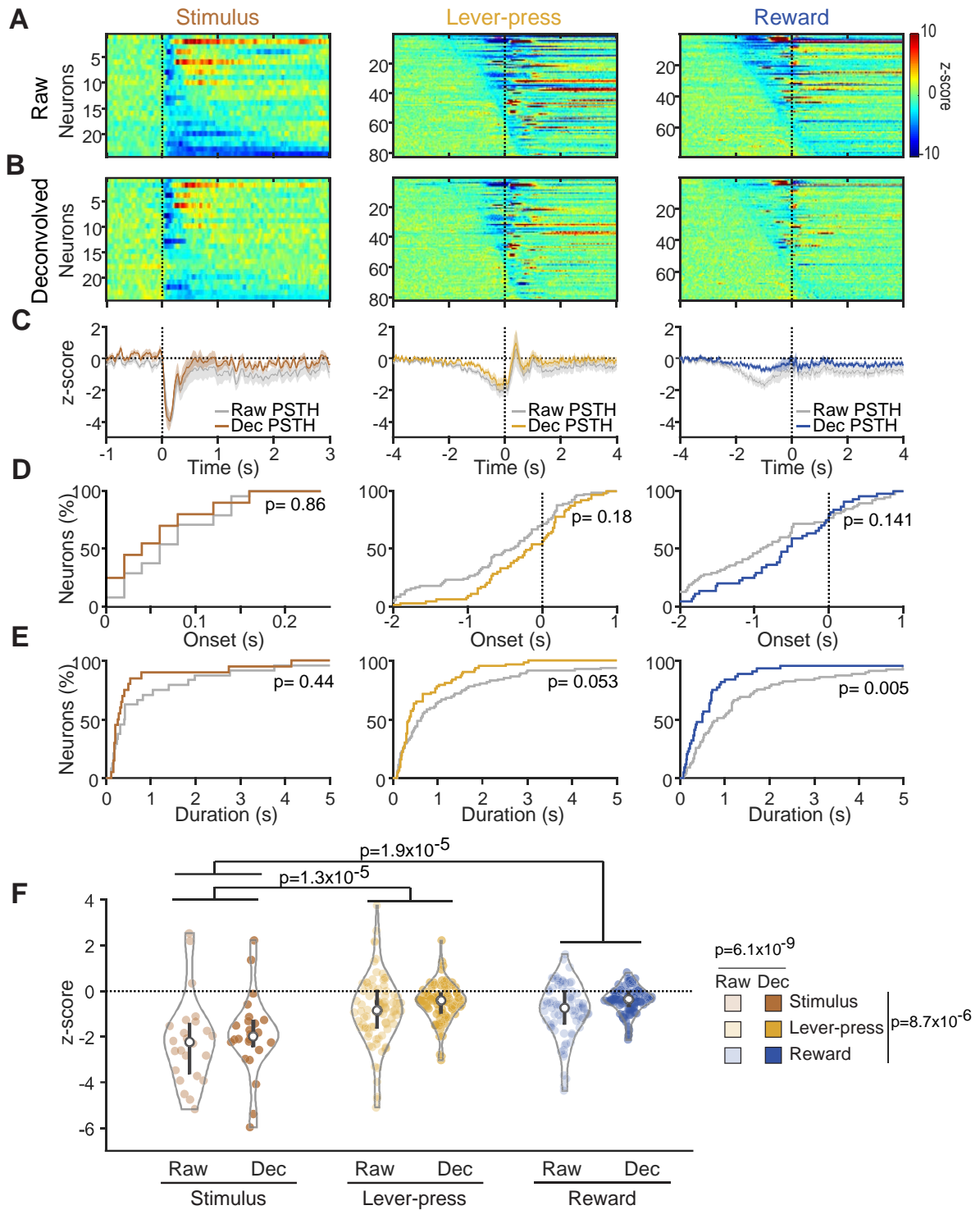


Figure 7

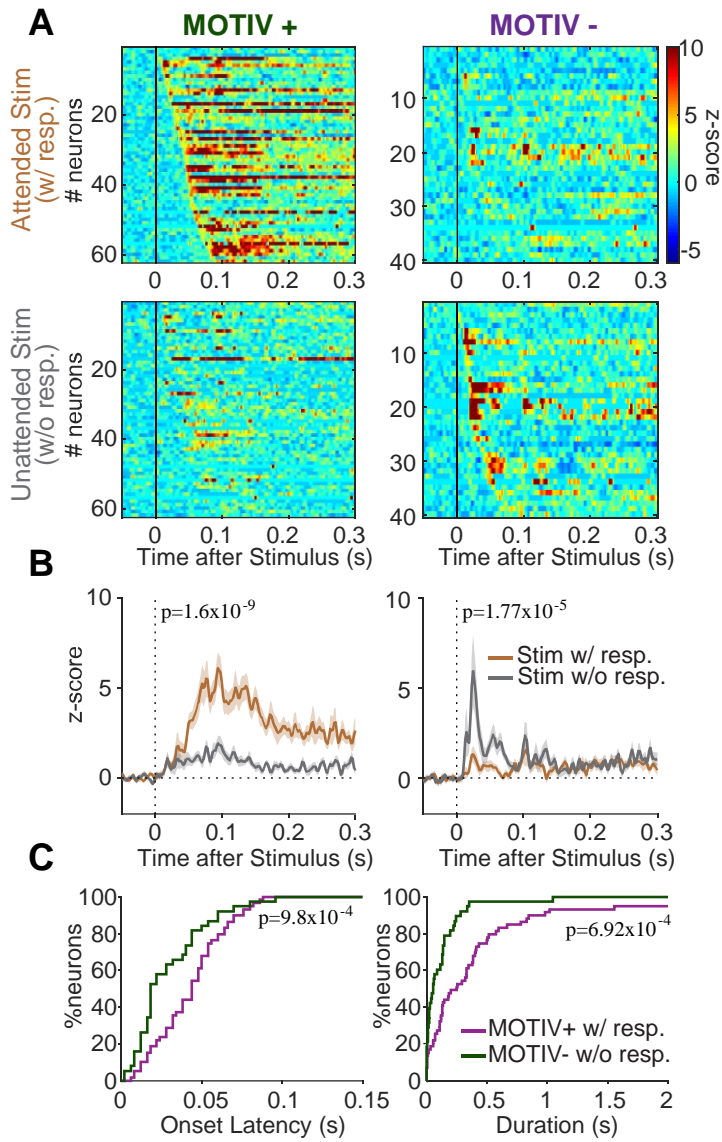
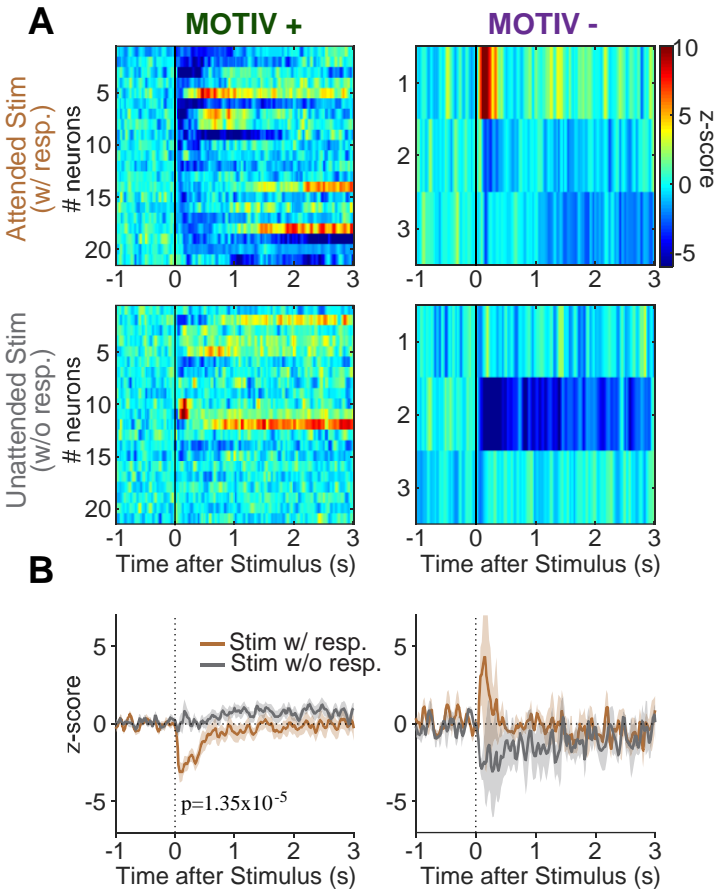
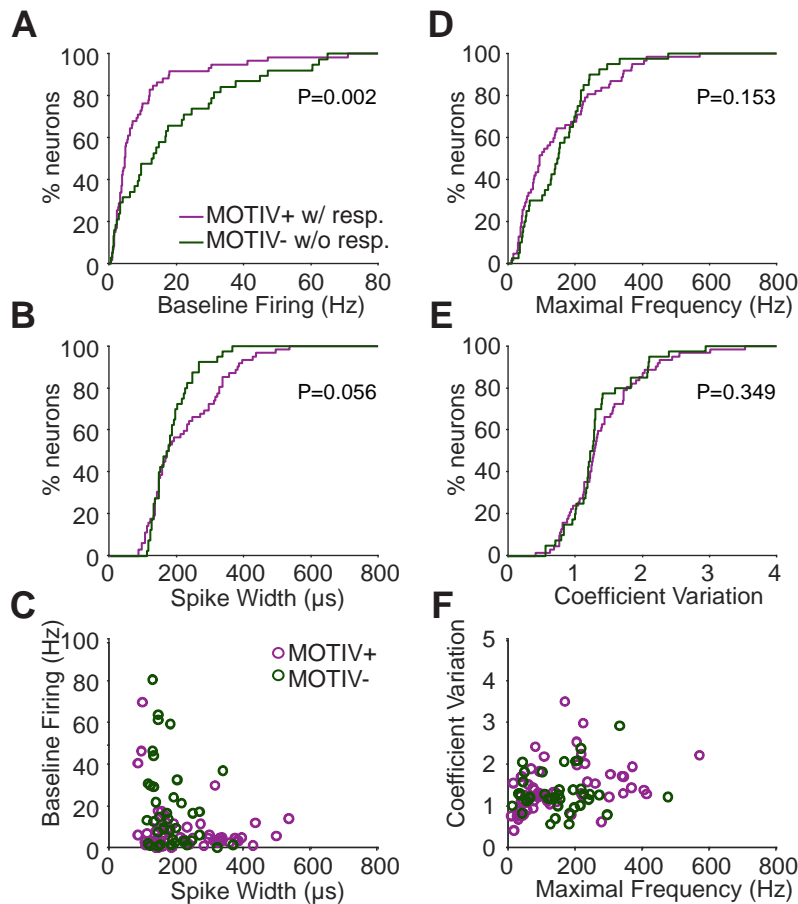


Figure 8



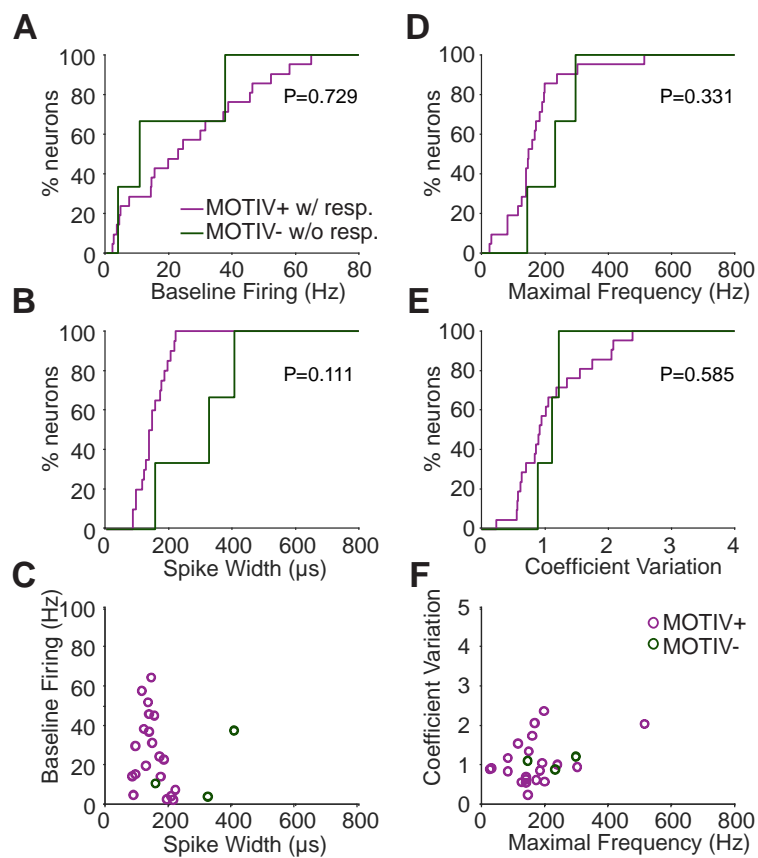
Supplementary Figure 1



Supplementary Fig.1. Electrophysiological characteristics of excited MOTIV+ and MOTIV- neurons.

A. Cumulative percentage of baseline firing rate of excited MOTIV+ (green) and excited MOTIV- (purple) neurons. **B.** Cumulative percentage of spike widths. **C.** Baseline firing rate plotted against spike width for individual neurons. **D.** Cumulative percentage of maximal frequencies. **E.** Cumulative percentage of the coefficients of variation. **F.** Coefficient of variation plotted against the maximal frequencies for individual neurons.

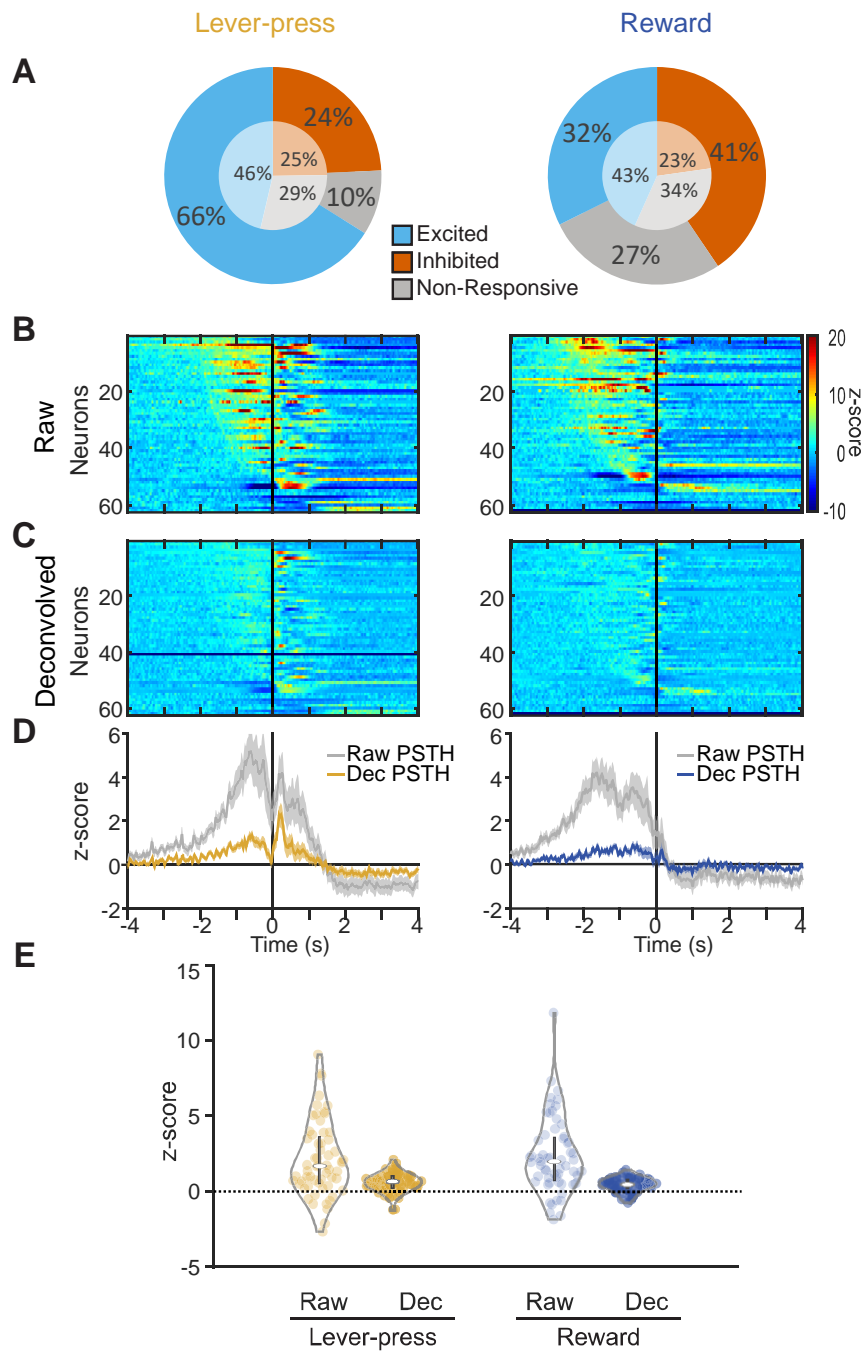
Supplementary Figure 2



Supplementary Fig.2. Electrophysiological characteristics of inhibited MOTIV+ and MOTIV- neurons.

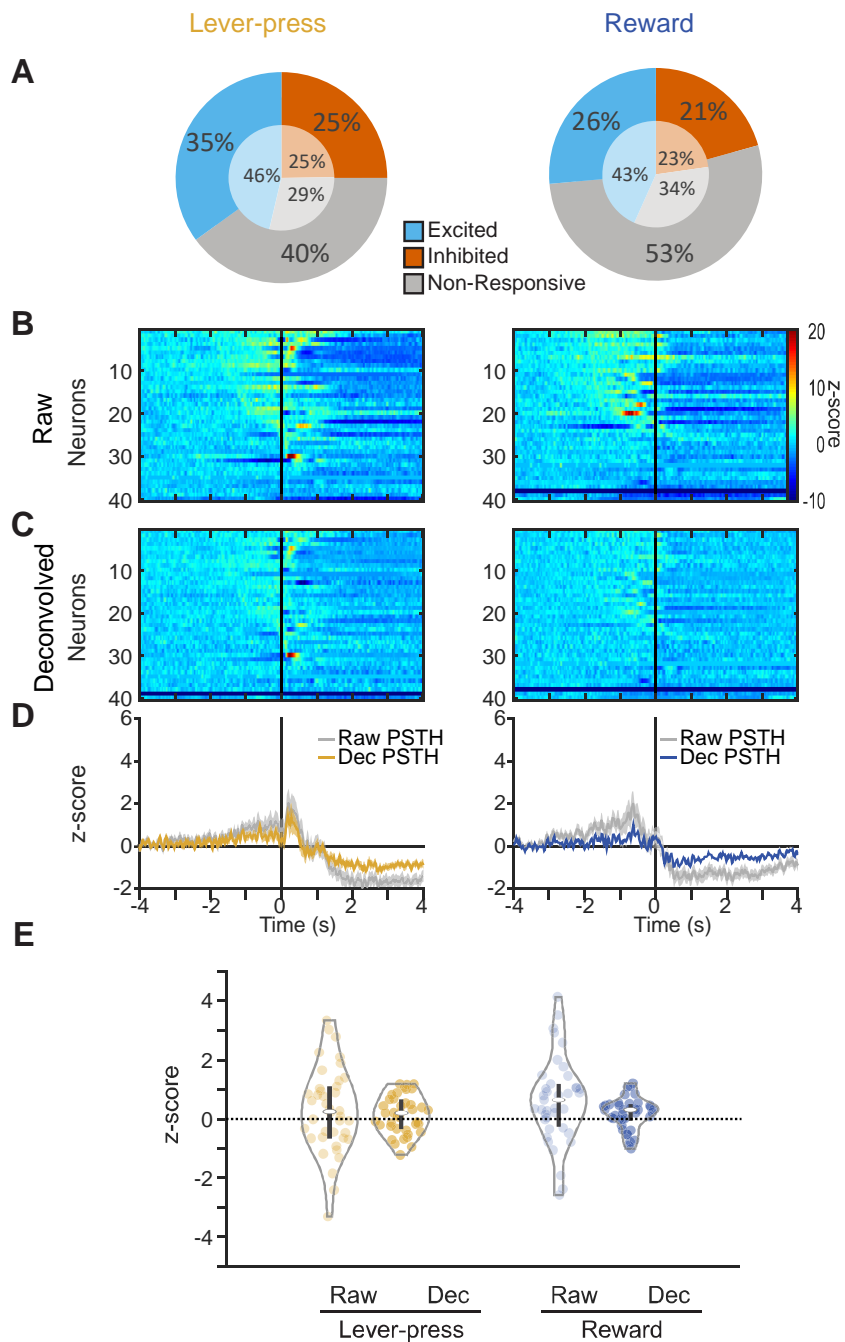
A. Cumulative percentage of baseline firing rate of inhibited MOTIV+ (green) and inhibited MOTIV- (purple) neurons. **B.** Cumulative percentage of spike widths. **C.** Baseline firing rate plotted against spike width for individual neurons. **D.** Cumulative percentage of maximal frequencies. **E.** Cumulative percentage of the coefficients of variation. **F.** Coefficient of variations plotted against the maximal frequencies for individual neurons.

Supplementary Figure 3



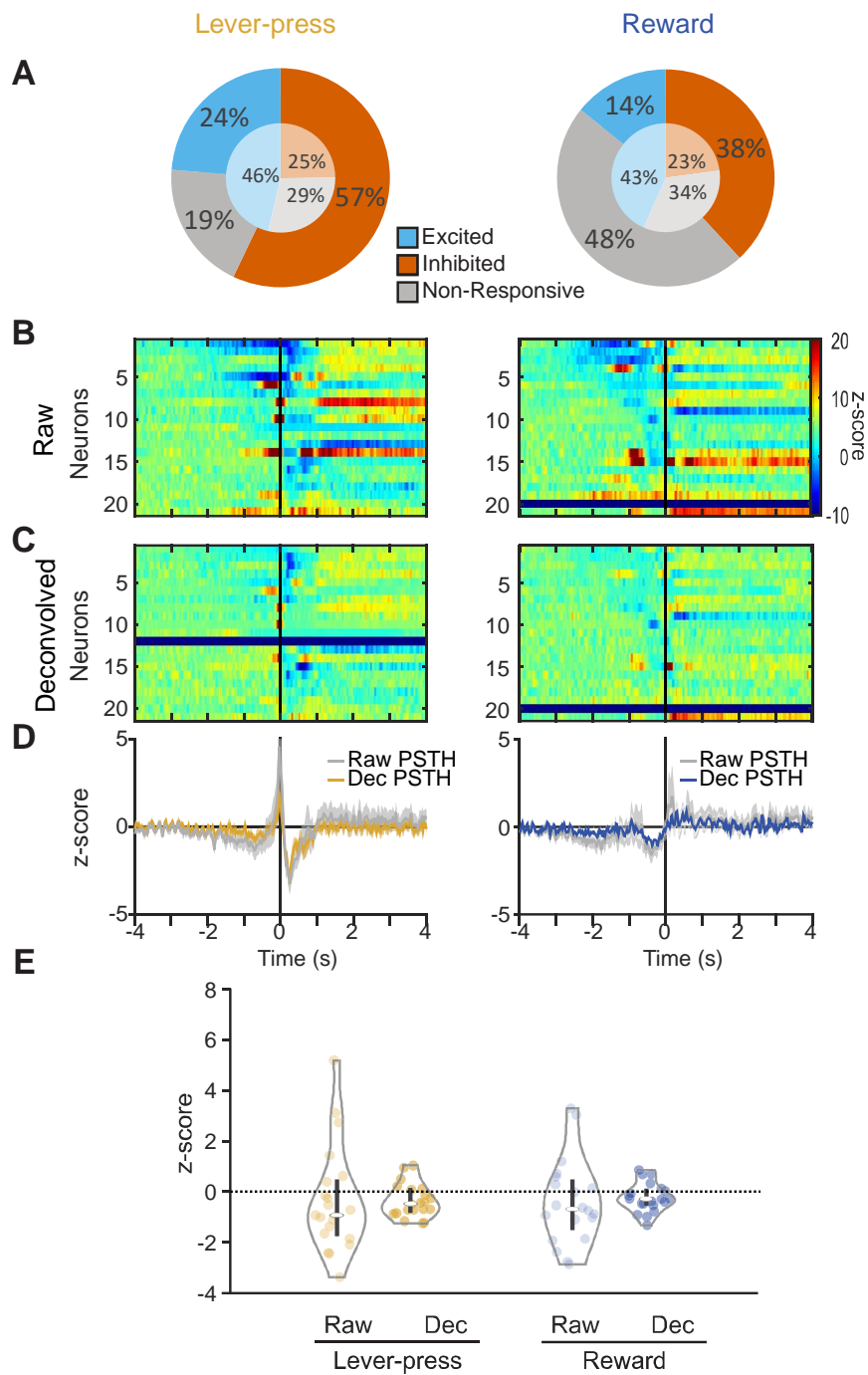
Supplementary Fig.3. Neuronal responses of Excited MOTIV+ neurons to lever-presses and reward deliveries. **A.** Proportion of excited, inhibited and non-responsive neurons for lever-presses (left) and reward deliveries (right). The internal pie charts represent the proportions of responses in the entire data set (n=399). The ring charts represent the same proportions for the population of excited MOTIV+ neurons. **B.** Heatmaps (top) and PSTHs (bottom). **C.** Violin plots of lever-press- and reward delivery-evoked firing.

Supplementary Figure 4



Supplementary Fig.4. Neuronal responses of excited MOTIV- neurons to lever-presses and reward deliveries. **A.** Proportion of excited, inhibited and non-responsive neurons for lever-presses (left) and reward deliveries (right). The internal pie charts represent the proportions of responses in the entire data set ($n=399$). The ring charts represent the same proportions for the population of excited MOTIV- neurons. **B.** Heatmaps (top) and PSTHs (bottom). **C.** Violin plots of lever-press- and reward delivery-evoked firing.

Supplementary Figure 5



Supplementary Fig.5. Neuronal responses of inhibited MOTIV+ neurons to lever-presses and reward deliveries. **A.** Proportion of excited, inhibited and non-responsive neurons for lever-presses (left) and reward deliveries (right). The internal pie charts represent the proportions of responses in the entire data set (n=399). The ring charts represent the same proportions for the population of inhibited MOTIV+ neurons. **B.** Heatmaps (top) and PSTHs (bottom). **C.** Violin plots of lever-press- and reward delivery-evoked firing.

Supplementary Table 1. Percentage and number (in parenthesis) of the different neuronal responses for individual rats.

Rat	n	Excited			Inhibited		
		Stimulus	Lever-Press	Reward	Stimulus	Lever-Press	Reward
1	139	39,6% (55)	53,2% (74)	52,5% (73)	5% (7)	18,7% (26)	21,6% (30)
2	65	20% (13)	53,8% (35)	50,8% (33)	10,8% (7)	30,8% (20)	27,7% (18)
3	66	53% (35)	60,6% (40)	59,1% (39)	4,5% (3)	9,1% (6)	6,1% (4)
4	51	56,9% (29)	66,7% (34)	68,6% (35)	2% (1)	21,6% (11)	21,6% (11)
5	14	28,6% (4)	50% (7)	57,1% (8)	14,3% (2)	42,9% (6)	28,6% (4)
6	4	75% (3)	75% (3)	75% (3)	0% (0)	25% (1)	0% (0)
7	60	26,7% (16)	60% (36)	61,7% (37)	6,7% (4)	20% (12)	18,3% (11)
Total	399	155	229	228	24	82	78

Supplementary Table 2. Percentage and number (in parenthesis) of the different neuronal response types for the stimulus, lever-press and reward delivery for raw and deconvolved data.

Stimulus	Lever-Press	Reward	Raw	Deconv.
Inhibited	Inhibited	Inhibited	3,8% (15)	1,8% (7)
Inhibited	Inhibited	No Resp.	0,3% (1)	0,8% (3)
Inhibited	Inhibited	Excited	0,5% (2)	0,5% (2)
Inhibited	No Resp.	Inhibited	0% (0)	0,3% (1)
Inhibited	No Resp.	No Resp.	0% (0)	1% (4)
Inhibited	No Resp.	Excited	0% (0)	0% (0)
Inhibited	Excited	Inhibited	0,3% (1)	0,8% (3)
Inhibited	Excited	No Resp.	0% (0)	0,8% (3)
Inhibited	Excited	Excited	1,3% (5)	2% (8)
No Resp.	Inhibited	Inhibited	7,8% (31)	4,8% (19)
No Resp.	Inhibited	No Resp.	1,3% (5)	2,5% (10)
No Resp.	Inhibited	Excited	2,8% (11)	4,5% (18)
No Resp.	No Resp.	Inhibited	2,8% (11)	2% (8)
No Resp.	No Resp.	No Resp.	14,8% (59)	25,1% (100)
No Resp.	No Resp.	Excited	2,5% (10)	3,3% (13)
No Resp.	Excited	Inhibited	1,8% (7)	1,8% (7)
No Resp.	Excited	No Resp.	3,8% (15)	4,5% (18)
No Resp.	Excited	Excited	17,8% (71)	12% (48)
Excited	Inhibited	Inhibited	2,3% (9)	1,8% (7)
Excited	Inhibited	No Resp.	0% (0)	0,8% (3)
Excited	Inhibited	Excited	2% (8)	4,8% (19)
Excited	No Resp.	Inhibited	0,5% (2)	0,5% (2)
Excited	No Resp.	No Resp.	1% (4)	3% (12)
Excited	No Resp.	Excited	0,5% (2)	0,8% (3)
Excited	Excited	Inhibited	1% (4)	2% (8)
Excited	Excited	No Resp.	1,5% (6)	2,8% (11)
Excited	Excited	Excited	30,1% (120)	15,5% (62)

Supplementary Table 3. Percentage and number (in parenthesis) of excited/inhibited MOTIV+/- neurons for individual rats.

Rat	n	Excited		Inhibited	
		MOTIV+	MOTIV-	MOTIV+	MOTIV-
1	139	18% (25)	5% (7)	3,6% (5)	0,7% (1)
2	65	15,4% (10)	10,8% (7)	6,2% (4)	3,1% (2)
3	66	7,6% (5)	12,1% (8)	6,1% (4)	0% (0)
4	51	23,5% (12)	21,6% (11)	3,9% (2)	0% (0)
5	14	7,1% (1)	0% (0)	7,1% (1)	0% (0)
6	4	25% (1)	0% (0)	0% (0)	0% (0)
7	60	13,3% (8)	11,7% (7)	8,3% (5)	0% (0)
Total	399	62	40	21	3